ELUCIDATING IMPACT-RELATED MAGNETIZATION ACQUISITION PROCESSES AT THE CHICXULUB CRATER WITH QUANTUM DIAMOND MICROSCOPY.

S. M. Tikoo[1,2,†], Y. Zhang[3,†], C. M. Verhagen[2], N. Swanson-Hysell[3], S. P. S. Gulick[4], D. A. Kring[5]. [1]Department of Geophysics, Stanford University, Stanford, CA 94305 (smtikoo@stanford.edu), [2]Department of Earth and Planetary Sciences, Rutgers University, Piscataway Township, NJ 08854, [3]Department of Earth and Planetary Science, University of California, Berkeley, 94720, [4]Institute for Geophysics, Jackson School of Geosciences, University of Texas at Austin, Austin, TX 78758, [5]Lunar and Planetary Institute, Universities Space Research Association, Houston, TX 77058, [†]Contributed equally.

Introduction: Impact cratering events are accompanied by intense shock waves, heating, and potentially post-impact hydrothermal activity that can lead to the acquisition of a complicated juxtaposition of shock remanent magnetization (SRM), thermoremanent magnetization (TRM), and chemical remanent magnetization (CRM) in crater rocks [1]. One challenge in interpreting the remanent magnetizations preserved in impactites is determining the nature and origin of the magnetic mineralogies that are responsible for carrying the different remanence components. The quantum diamond microscope (QDM), which allows for nitrogen vacancy magnetometry to be applied to paleomagnetic studies, provides an avenue for addressing this problem thanks to its ability to image magnetic fields with ~μm-scale resolution [2]. We pair QDM maps and scanning electron microscope (SEM) images to locate magnetic sources and elucidate that at least two distinct populations of remanence carriers exist in the 66 Ma Chicxulub crater impactites drilled in 2016.

Samples and Methods: We studied the paleomagnetism of several Chicxulub peak ring samples obtained from International Ocean Discovery Program (IODP) and International Continental Scientific Drilling Program (ICDP) Expedition 364 [3,4]. We analyzed extensively hydrothermally altered impact melt-bearing breccias (suevites from cores 47R2, 50R2, 53R3, 54R1, and 68R1), an impact melt rock (93R1), a granitic cataclasite (184R1), and a basement granite (240R3). In this abstract, we focus on suevites and impact melt rocks from the Chicxulub upper peak ring.

We prepared 2.5 cm diameter mini-cores from each sample. The NRM of each mini-core was measured and subsequently stepwise demagnetized by alternating fields (AF) using a superconducting magnetometer. Magnetization component directions were fit via principal component analysis [5]. 1 to 3 ~30-μm-thick thin sections were prepared from adjacent sister specimens of each mini-core. Thin sections were inspected using reflected light to identify regions that contain visible iron oxides. We then conducted QDM measurements of these thin sections to produce ~1.2 x 1.5 mm rectangular magnetic maps of selected regions. Afterward, we collected backscattered SEM images of strongly magnetic areas within samples and measured magnetic mineral compositions with energy-dispersive X-ray spectroscopy (EDS).

Results:

Suevites. Bulk sample AF demagnetization results show that suevite samples typically contain low coercivity (LC) overprints, prominent but non-origin-trending medium coercivity (MC) components, and (sometimes non-origin-trending) high coercivity (HC) components with lower magnitudes and varying directions. Some MC components have inclination values similar to the expected ~-44° paleofield inclination at Chicxulub at the time of impact (assuming an axial dipole field).

QDM measurements revealed two populations of strongly magnetic sources. In coarse-grained suevite sample 68R1 (MC inclination 30.8±4.5°), we observed a small (0.75 cm x 0.25 cm) clast with a relatively unaltered appearance that contained strongly magnetic, isolated iron oxide grains. In the same sample, >100 μm-diameter clusters of smaller iron oxide grains individually ranging from ~1 μm to ~20 μm in diameter were visible within fractures, void spaces, and alteration veins interior to a ~1 cm diameter clast with a highly shocked and altered appearance (**Fig. 1**).

Our SEM images reveal that iron oxide grains within these clusters are euhedral and we interpret them to be hydrothermal in origin [6]. The complex magnetic field patterns in our QDM maps of these clusters are consistent with the interpretation that discrete magnetic grains within clusters have overlapping magnetic fields. We observed nearly identical clusters within fractured clasts in finer-grained suevite (clast diameters <5 mm) samples 50R2 (MC inclination -41.4±4.7°) and 47R2 (MC inclination -14.3±6.0°). Magnetizations of clusters can have intensities comparable to and sometimes higher than primary iron oxide grains in the aforementioned unaltered clast, even to the point of exceeding the QDM measurement threshold in some cases. Other clast-held remanences were observed in fine-grained suevite samples 47R2 and 53R3, but further microscopy is needed to ascertain whether or not the magnetic grains within them are primary or hydrothermal in origin. Isolated and mostly weakly magnetic sources were sometimes observed elsewhere (within both clasts and matrix).

Hydrothermally-produced iron sulfides of various morphologies are abundant throughout the suevite samples [4], although none of these were magnetic. EDS measurements demonstrate that most of the hydrothermal oxides have high Fe/Ti ratios, indicating

they are nearly pure magnetite. However, some grains (particularly at cluster edges) have higher Ti contents and may be maghemite or hematite. The higher-Ti grains often exhibit a platy morphology.

Impact melt rocks. Peak ring impact melt rock sample 93R1 has a single-component, high-coercivity remanence with an inclination of -40.4±1.7°, which is close to the -44° expected value at the time of impact (assuming a geocentric axial dipole field). Our QDM maps of 93R1 suggest that the dominant magnetization carriers within impact melt rocks are ultrafine-grained iron oxides (likely titanomagnetite) that are distributed relatively homogeneously throughout a melt glass matrix. The oxides are too small for EDS compositional analysis. There are localized regions within impact melt rocks that appear devoid of magnetic sources that may represent Fe-poor carbonate melt.

Discussion and Conclusions: We found that many of the strongest magnetic carriers in Chicxulub suevite samples were clusters of hydrothermally-grown, Ti-poor, magnetite grains that formed within alteration veins and vugs within shock-fractured clasts of likely igneous origin. Using the QDM to obtain a bulk-scale magnetization direction would require independently imaging very large numbers of magnetic grains. However, given that clusters are orders of magnitude more magnetic than the background and suevite matrix, it is likely that CRM is a significant source of magnetization in this lithologic group, even for samples whose magnetization directions do not perfectly coincide with the expected paleofield orientation at the time of the Chicxulub impact. Primary Fe-Ti oxides within reworked igneous basement or impact melt clasts may also carry remanence but given that these would be randomly reoriented prior to suevite emplacement, their overall contributions to the bulk sample magnetizations are expected to be small. Different suevite samples may have different ratios of CRM and pre-depositional clast magnetizations, with overlapping coercivities and unblocking temperatures, resulting in dispersed magnetic inclinations between samples as reported by [4]. Impact melt rock matrices do not appear to contain hydrothermal magnetite. Magnetic sources within impact melt rocks are <1 μm titanomagnetite grains distributed throughout the melt glass matrix that likely preserve TRM from primary cooling. Ongoing work will address the nature of magnetization preserved in uplifted basement rocks and cataclasites.

References: [1] Gilder, S. A. et al. (2018) "Magnetic signatures of terrestrial meteorite impact craters: A summary", *Magnetic Fields in the Solar System.* Springer, Cham, 357-382. [2] Glenn D. R. et al. (2017) *Geochem. Geophys. Geosys.*, *18*, 3254-3267. [3] Morgan J. V. et al. (2016) *Science*, *354*(6314), 878-882. [4] Kring, D. A. et al. (2020) *Sci. Adv.*, *6*, eaaz3053. [5] Kirschvink J. L. (1980) *Geophys. J. Roy. Astr. S., 62,* 699-718. [6] Eliopoulos D. G. and Economou-Eliopoulous M. (2019) *Minerals*, *9*, 759.
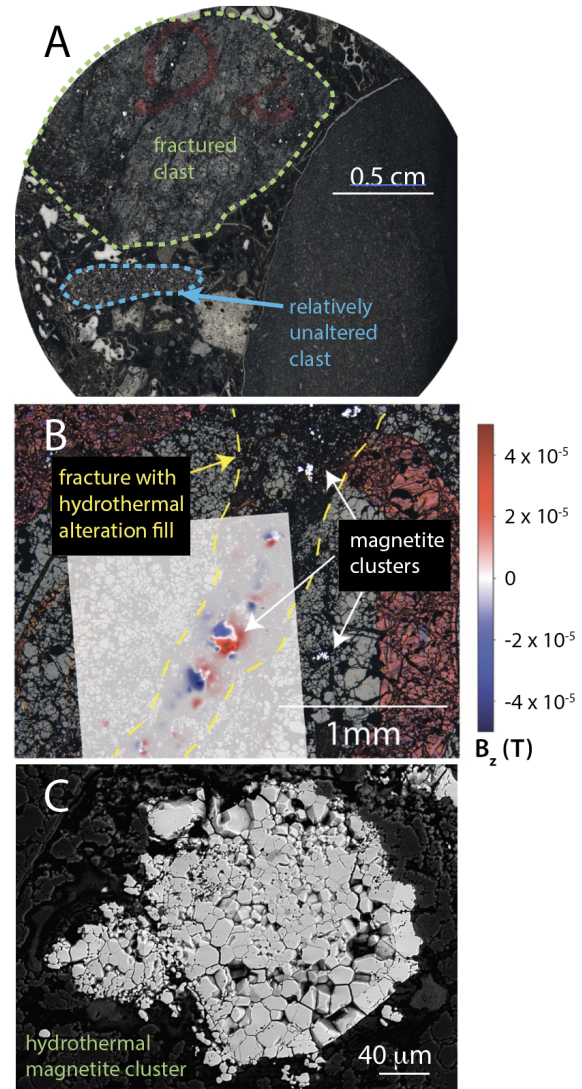

Fig. 1. Imaging of magnetic minerals within coarse-grained suevite sample 68R1. (A) Thin section reflected light image showing the fractured, heavily altered clast and the relatively unaltered clast described in the text. (B) QDM magnetic map of magnetite clusters located within the hydrothermally altered fracture encircled in red marker at the top of part A. (C) BSEM image of a hydrothermally precipitated magnetite cluster.